Enhanced Sequence Specific Recognition in the Minor Groove of DNA by Covalent Peptide Dimers: Bis(pyridine-2-carboxamidonetropsin)$(CH_2)_{3-6}$

Milan Mrksich and Peter B. Dervan*

Contribution from the Arnold and Mabel Beckman Laboratories of Chemical Synthesis, California Institute of Technology, Pasadena, California 91125

Received May 28, 1993®

Abstract: The designed peptide pyridine-2-carboxamidonetropsin (2-PyN) binds to the minor groove of double-helical DNA at two very different sequences, 5′-TTTTT-3′ and 5′-TGTCA-3′, with comparable energetics but quite different structures. 2-PyN likely binds the 5′-TTTTT-3′ site as a 1:1 complex, whereas 2-PyN binds 5′-TGTCA-3′ sites as a 2:1 complex. In order to enhance the binding affinity of 2-PyN for the 5′-TGTCA-3′ site, covalently linked dimers of 2-PyN have been synthesized wherein the nitrogens of the central pyrroles are connected with propyl, butyl, pentyl, and hexyl linkers. DNase I footprint titration experiments reveal that these bis(pyridine-2-carboxamidenetropsin)$(CH_2)_{3-6}$ peptides bind to a 5′-TGTCA-3′ site with binding affinities 10-fold greater than that of 2-PyN. By taking advantage of the different structures of peptides bound in the minor groove, the ratio of binding affinities of 2-PyN for 5′-TGTCA-3′ and 5′-TTTTT-3′ sites have been altered from 1:1 to 25:1.

1:1 and 2:1 Peptide–DNA Complexes. The natural products netropsin and distamycin A are crescent shaped di- and tripeptides, respectively, that bind in the minor groove of DNA at sites of four or five successive A,T base pairs (bp).[1-3] The structures of a number of peptide–DNA complexes have been determined by X-ray diffraction[4] and NMR spectroscopy,[5] and the thermodynamic profiles have been studied for these complexes.[6] This work suggests that favorable electrostatic interactions and extensive van der Waals contacts between the peptide and the floor and walls of the minor groove contribute to complex stability. The carboxamide NH's of the peptides participate in bifurcated hydrogen bonds with adenine N3 and thymide O2 atoms on the floor of the minor groove. The aromatic hydrogens of the *N*-methylpyrrole rings are set too deeply in the minor groove to allow room for the guanine 2-amino group of a G,C base pair, affording binding specificity for A,T-rich sequences. Although this model has aided in the design of oligopeptides for recognition of longer tracts of A,T-rich DNA,[7] efforts to design peptides capable of binding mixed A,T and G,C sequences have proven inconsistent with a 1:1 peptide–DNA model.[8,9]

There have been several recent reports of peptides which bind in the minor groove of DNA as antiparallel side-by-side dimers.[10-15] Pelton and Wemmer found that distamycin at high concentrations (2–4 mM) is capable of binding in the minor groove of 5′-AAATT-3′ as a dimer.[10] Shortly thereafter, the designed peptide 1-methylimidazole-2-carboxamidonetropsin (2-ImN) was shown to bind exclusively to the mixed sequence 5′-TGTCA-3′ as a 2:1 complex.[11,12] Another synthetic peptide analog pyridine-2-carboxamidonetropsin (2-PyN) was found to bind to the minor groove of double-helical DNA at two very different sequences, 5′-TTTTT-3′ and 5′-TGTCA-3′.[9,11] From quantitative footprint titration experiments, the apparent first-order binding affinities for 2-PyN in complex with 5′-TTTTT-3′ and 5′-TGTCA-3′ are comparable, $K_a = 2.3 \times 10^5$ and 2.7×10^5 M^{-1}, respectively (20 mM Tris·HCl and 100 mM NaCl at pH 7.0 and 37 °C).[16] 2-PyN likely binds 5′-TTTTT-3′ as a 1:1 complex and 5′-TGTCA-3′ as a 2:1 complex (Figure 1).

Experimental Design. One strategy for increasing the affinity and hence the sequence specificity of peptides that bind DNA sites as side-by-side dimers in the minor groove is to covalently tether the two peptides.[17] The overall free energy of complex formation is expected to be more favorable for a covalent dimer since one bis-peptide should bind with more favorable entropy than do two peptides. Examination of 2:1 peptide–DNA models

® Abstract published in *Advance ACS Abstracts*, October 1, 1993.

(1) (a) Krylov, A. S.; Grokhovsky, S. L.; Zasedatelev, A. S.; Zhuze, A. L.; Gursky, G. V.; Gottikh, B. P. *Nucl. Acids. Res.* **1979**, *6*, 289–304. (b) Zasedatelev, A. S.; Gursky, G. V.; Zimmer, Ch.; Thrum, H. *Mol. Biol. Rep.* **1974**, *1*, 337–342. (c) Zasedatelev, A. S.; Zhuze, A. L.; Zimmer, Ch.; Grokhovsky, S. L.; Tumanyan, V. G.; Gursky, G. V.; Gottikh, B. P. *Dokl. Acad. Nauk SSSR* **1976**, *231*, 1006–1009. For a review, see: (d) Zimmer, C.; Wähnert, U. *Prog. Biophys. Molec. Biol.* **1986**, *47*, 31–112.

(2) (a) Van Dyke, M. W.; Hertzberg, R. P.; Dervan, P. B. *Proc. Natl. Acad. Sci. U.S.A.* **1982**, *79*, 5470–5474. (b) Van Dyke, M. W.; Dervan, P. B. *Cold Spring Harbor Symposium on Quantitative Biology* **1982**, *47*, 347–353. (c) Van Dyke, M. W.; Dervan, P. B. *Biochemistry* **1983**, *22*, 2373–2377. (d) Harshman, K. D.; Dervan, P. B. *Nucl. Acids Res.* **1985**, *13*, 4825–4835. (e) Fox, K. R.; Waring, M. J. *Nucl. Acids Res.* **1984**, *12*, 9271–9285. (f) Lane, M. J.; Dobrowiak, J. C.; Vournakis, J. *Proc. Natl. Sci. U.S.A.* **1983**, *80*, 3260–3264.

(3) (a) Schultz, P. G.; Taylor, J. S.; Dervan, P. B. *J. Am. Chem. Soc.* **1982**, *104*, 6861–6863. (b) Taylor, J. S.; Schultz, P. G.; Dervan, P. B. *Tetrahedron* **1984**, *40*, 457–465. (c) Schultz, P. G.; Dervan, P. B. *J. Biomol. Struct. Dyn.* **1984**, *1*, 1133–1147. (d) Dervan, P. B. *Science* **1986**, *232*, 464–471.

(4) (a) Kopka, M. L.; Yoon, C.; Goodsell, D.; Pjura, P.; Dickerson, R. E. *Proc. Natl. Acad. Sci. U.S.A.* **1985**, *82*, 1376–1380. (b) Kopka, M. L.; Yoon, C.; Goodsell, D.; Pjura, P.; Dickerson, R. E. *J. Mol. Biol.* **1985**, *183*, 553–563. (c) Coll, M.; Frederick, C. A.; Wang, A. H.-J.; Rich, A. *Proc. Natl. Acad. Sci. U.S.A.* **1987**, *84*, 8385–8389.

(5) (a) Patel, D. J.; Shapiro, L. *J. Biol. Chem.* **1986**, *261*, 1230–1240. (b) Klevitt, R. E.; Wemmer, D. E.; Reid, B. R. *Biochemistry* **1986**, *25*, 3296–3303. (c) Pelton, J. G.; Wemmer, D. E. *Biochemistry* **1988**, *27*, 8088–8096.

(6) (a) Markey, L. A.; Breslauer, K. J. *Proc. Natl. Acad. Sci. U.S.A.* **1987**, *84*, 4359–4363. (b) Breslauer, K. J.; Remeta, D. P.; Chou, W.-Y.; Ferrante, R.; Curry, J.; Zaunczkowski, D.; Snyder, J. G.; Marky, L. A. *Proc. Natl. Acad. Sci. U.S.A.* **1987**, *84*, 8922–8926.

(7) Dervan, P. B. *Science* **1986**, *232*, 464–471.

(8) (a) Lown, J. W.; Krowicki, K.; Bhat, U. G.; Ward, B.; Dabrowiak, J. C. *Biochemistry* **1986**, *25*, 7408–7416. (b) Kissinger, K.; Krowicki, K.; Dabrowiak, J. C.; Lown, J. W. *Biochemistry* **1987**, *26*, 5590–5595.

(9) Wade, W. S.; Dervan, P. B. *J. Am. Chem. Soc.* **1987**, *109*, 1574–1575.

(10) (a) Pelton, J. G.; Wemmer, D. E. *Proc. Natl. Acad. Sci. U.S.A.* **1989**, *86*, 5723–5727. (b) Pelton, J. G.; Wemmer, D. E. *J. Am. Chem. Soc.* **1990**, *112*, 1393–1399.

(11) Wade, W. S.; Mrksich, M.; Dervan, P. B. *J. Am. Chem. Soc.* **1992**, *114*, 8783–8794.

(12) Mrksich, M.; Wade, W. S.; Dwyer, T. J.; Geierstanger, B. H.; Wemmer, D. E.; Dervan, P. B. *Proc. Natl. Acad. Sci. U.S.A.* **1992**, *89*, 7586–7590.

(13) Dwyer, T. J.; Geierstanger, B. H.; Bathini, Y.; Lown, J. W.; Wemmer, D. E. *J. Am. Chem. Soc.* **1992**, *114*, 5911–5919.

(14) Mrksich, M.; Dervan, P. B. *J. Am. Chem. Soc.* **1993**, *115*, 2572–2576.

(15) Geierstanger, B. H.; Jacobsen, J.-P.; Mrksich, M.; Dervan, P. B.; Wemmer, D. E. Manuscript in preparation.

(16) Wade, W. S.; Mrksich, M.; Dervan, P. B. *Biochemistry* In press.

0002-7863/93/1515-9892$04.00/0

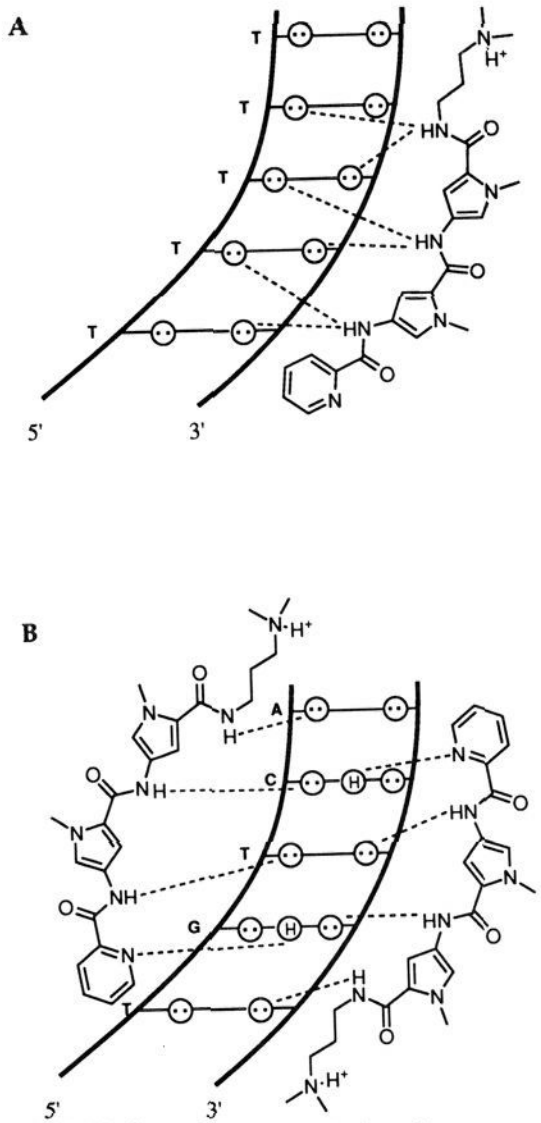

Figure 1. (a) 1:1 binding model for the complex formed between 2-PyN with a 5′-TTTTT-3′ sequence, with the nitrogen of the pyridine facing away from the minor groove and (b) 2:1 binding model for the dimeric complex formed between 2-PyN with a 5′-TGTCA-3′ sequence, with the nitrogens of the pyridines facing the floor of the minor groove. Circles with dots represent lone pairs of N3 of purines and O2 of pyrimidines and circles with an H represent the 2-amino group of guanine. Putative hydrogen bonds are illustrated by dotted lines.

suggest that linkers from three to six methylene units are able to bridge the central pyrrole rings of the two side-by-side peptides in complex with DNA without perturbing the contacts between the peptides and DNA (Figure 2).[10,12] Four covalently linked dimers of 2-PyN have been synthesized wherein the peptides are connected through the nitrogens of the central pyrrole rings with propyl, butyl, pentyl, and hexyl linkers (Figure 3). DNase I footprint titration experiments with these bis(pyridine-2-carboxamidenetropsin)$(CH_2)_{3-6}$ peptides afford a comparison of the binding affinities of 2-PyN and the four covalent peptide dimers $(2\text{-PyN})_2$-C3, $(2\text{-PyN})_2$-C4, $(2\text{-PyN})_2$-C5, and $(2\text{-PyN})_2$-C6 to both the 5′-TTTTT-3′ and 5′-TGTCA-3′ sites.

(17) For examples of end-to-end linked peptides, see: (a) Schultz, P. G.; Dervan, P. B. *J. Am. Chem. Soc.* **1983**, *105*, 7748–7750. (b) Youngquist, R. S.; Dervan, P. B. *J. Am. Chem. Soc.* **1985**, *107*, 5528–5529. (c) Griffin, J. H.; Dervan, P. B. *J. Am. Chem. Soc.* **1986**, *108*, 5008–5009. (d) Griffin, J. H.; Dervan, P. B. *J. Am. Chem. Soc.* **1987**, *109*, 6840–6842. (e) Youngquist, R. S.; Dervan, P. B. *J. Am. Chem. Soc.* **1987**, *109*, 7564–7566.

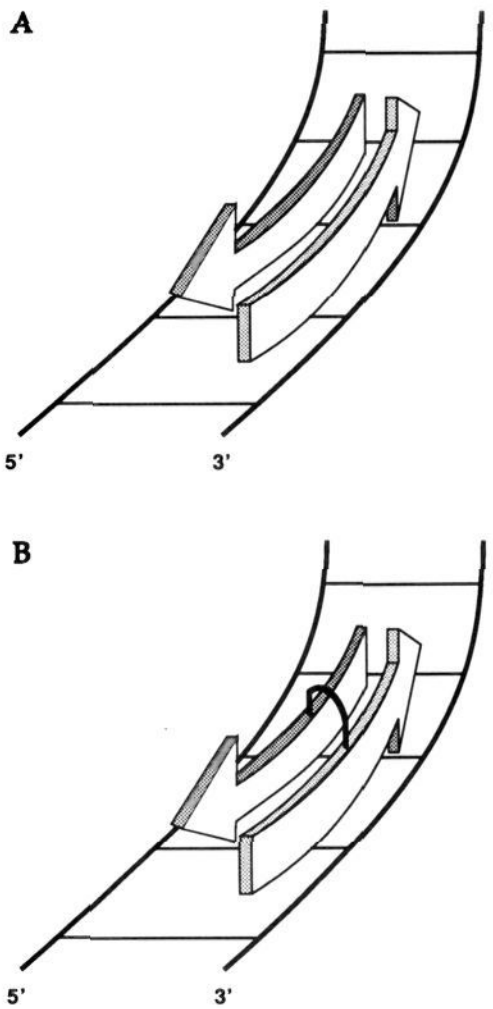

Figure 2. Models for (a) binding of two antiparallel side-by-side peptides and (b) binding by a single covalent peptide dimer in the minor groove of DNA.

Results

Synthesis of Covalently Linked Peptides. The methodology for the synthesis of covalently linked peptides is analogous to that of the corresponding monomeric peptides (Figure 4).[11] Alkylation of 4-nitro-2-(carboxymethyl)pyrrole with a diiodoalkane (K_2CO_3, acetone) affords the corresponding di-*N*,*N*′-pyrrolealkanes **2a–d** in 80–85% yield. Saponification of the methyl esters (LiOH, EtOH, and H_2O) followed by conversion to the bis(acid chlorides) ($SOCl_2$) and coupling with 1-methyl-4-amino-2-(carboxamidopropyl)-3-(dimethylamino)pyrrole yields the corresponding bis-dipyrrole derivatives **4a–d** in 50–70% yield. Reduction of the bis-nitrodipyrroles (300 psi H_2, Pd/C) and coupling of the resulting bis-aminopyrroles with picolinic acid (DCC, HOBt) affords the dimeric peptides $(2\text{-PyN})_2$-C3, $(2\text{-PyN})_2$-C4, $(2\text{-PyN})_2$-C5, and $(2\text{-PyN})_2$-C6 in 45–60% yield.

DNase I Footprinting. DNase I footprinting experiments on the 517-bp *Eco*R I/*Rsa* I restriction fragment from plasmid pBR322 (10 mM Tris·HCl, 10 mM KCl, 10 mM $MgCl_2$, 5 mM $CaCl_2$, and 100 μM-bp calf thymus DNA at pH 7.0 and 22 °C) reveal that 2-PyN and the covalent peptide dimers $(2\text{-PyN})_2$-C3, $(2\text{-PyN})_2$-C4, $(2\text{-PyN})_2$-C5, and $(2\text{-PyN})_2$-C6, at 40 μM concentration, protect both the 5′-TGTCA-3′ and the 5′-TTTTT-3′ sites from cleavage by the enzyme DNase I (Figure 5, lanes 4–9).[18] At 10 μM concentration, 2-PyN does not protect any sites on double-helical DNA from cleavage by DNase I (Figure 5, lane 10). In contrast, the covalently linked peptides, $(2\text{-PyN})_2$-C3,

(18) (a) Galas, D.; Schmitz, A. *Nucl. Acids. Res.* **1978**, *5*, 3157–3170. (b) Fox, K. R.; Waring, M. J. *Nucl. Acids Res.* **1984**, *12*, 9271–9285.

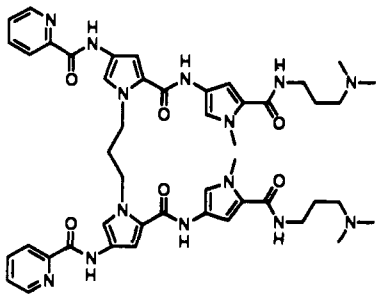

1a: (2-PyN)$_2$-C3

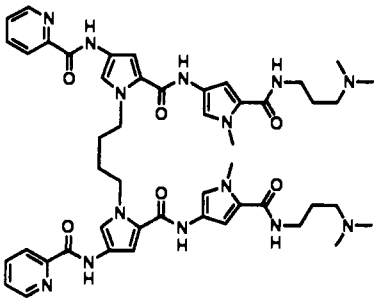

1b: (2-PyN)$_2$-C4

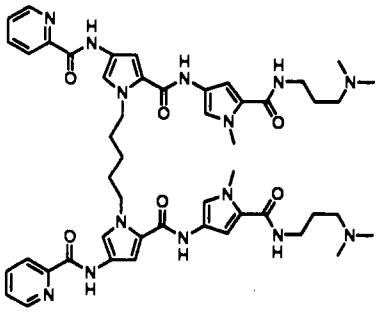

1c: (2-PyN)$_2$-C5

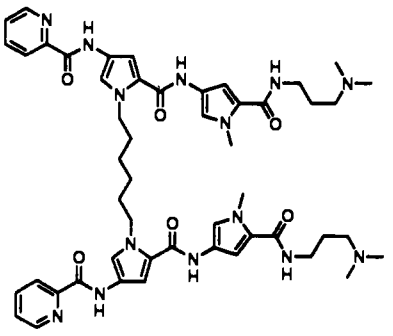

1d: (2-PyN)$_2$-C6

Figure 3. Covalently linked peptide dimers (2-PyN)$_2$-C3, (2-PyN)$_2$-C4, (2-PyN)$_2$-C5, and (2-PyN)$_2$-C6 wherein the central pyrroles of 2-PyN are connected with propyl, butyl, pentyl, and hexyl linkers, respectively.

(2-PyN)$_2$-C4, (2-PyN)$_2$-C5, and (2-PyN)$_2$-C6, at 10 μM concentration, do bind the 5′-TGTCA-3′ site (Figure 5, lanes 11–14). In order to compare the binding affinities of the five peptides in complex with the 5′-TGTCA-3′ and 5′-TTTTT-3′ sites, the relative binding affinities were determined by DNase I footprint titration experiments (Table I).[19] All four covalently linked peptides bind the 5′-TGTCA-3′ site with apparent first order binding constants approximately one order of magnitude greater than that of 2-PyN. The (2-PyN)$_2$-C3 and (2-PyN)$_2$-C4 peptides bind to the A,T-rich site with slightly lower affinities than does 2-PyN, while (2-PyN)$_2$-C5 and (2-PyN)$_2$-C6 bind to this site with affinities comparable to that of the parent peptide 2-PyN (Table I).

Table I. Relative Binding Affinities[a,b]

peptide	binding site 5′-TGTCA-3′	binding site 5′-TTTTT-3′
2-PyN	1.2	1.0
(2-PyN)$_2$-C3	10.0	0.5
(2-PyN)$_2$-C4	13.3	0.5
(2-PyN)$_2$-C5	8.8	1.2
(2-PyN)$_2$-C6	6.7	1.2

[a] Values reported are ratios of binding affinities relative to that for 2-PyN binding the 5′-TTTTT-3′ site. [b] The assays were performed in the presence of 10 mM Tris·HCl, 10 mM KCl, 10 mM $MgCl_2$, 5 mM $CaCl_2$, and 100 μM-bp calf thymus DNA at pH 7.0 and 22 °C.

Discussion

Binding Affinity. The DNase I footprinting experiments reveal that the binding affinities of the covalently linked dimers in complex with the 5′-TGTCA-3′ site are 10-fold greater than that of the parent peptide 2-PyN in complex with this site. Covalently tethering the two peptides therefore results in more favorable free energies of binding, likely due to more favorable entropies of binding. A comparison of the relative binding affinities for the 5′-TGTCA-3′ site by the covalently linked peptides suggests that the length of the alkyl linker has little effect on overall complex stability. Because these simple alkyl linkers may not be optimized for side-by-side binding, a second generation of linked peptides may display still higher affinities for dimeric binding sites. With regard to binding the 5′-TTTTT-3′ site, all four covalently linked peptide dimers bind with affinities comparable to that for 2-PyN. If one peptide of the covalently linked dimer is bound in the minor groove of the A,T-rich site, we would expect the steric bulk of the other peptide to destabilize the complex. Consistent with this interpretation, the linked peptides with the shorter propyl and butyl tethers display lower binding affinity for the A,T-rich site relative to the peptides with the longer pentyl and hexyl linkers. Thermodynamic studies may provide further insight into the enthalpy–entropy compensations in these complexes.

Sequence Specificity. The four covalent dimers all display increased sequence specificities relative to the parent compound 2-PyN (Figure 6). The monomeric peptide 2-PyN binds the A,T-rich site and the 5′-TGTCA-3′ site with similar binding affinities and consequently displays little discrimination between these two sites. The covalently linked peptides, however, bind the 5′-TGTCA-3′ site with 5–25-fold higher affinties relative to binding the 5′-TTTTT-3′ site (Figure 6 and Table I). Moreover, this difference in stabilities mainly arises from *enhanced binding to the 5′-TGTCA-3′ site*, rather than decreased binding affinities for the 5′-TTTTT-3′ site.

Binding Models. Although the footprint titrations suggest that the covalent peptide dimers bind the 5′-TGTCA-3′ site as intramolecular dimers, there remains the possibility of intermolecular dimeric binding by two covalently linked peptides. In collaboration with the Wemmer group, we have studied the complexes of 2-PyN and the four covalent peptide dimers with an oligonucleotide containing a 5′-TGACT-3′ binding site by two-dimensional NMR.[20] In all cases, one-dimensional spectra of titration experiments of the oligonucleotide with increasing

(19) (a) Brenowitz, M.; Senear, D. F.; Shea, M. A.; Ackers, G. K. *Methods Enzymol.* **1986**, *130*, 132–181. (b) Brenowitz, M.; Senear, D. F.; Shea, M. A.; Ackers, G. K. *Proc. Natl. Acad. Sci. U.S.A.* **1986**, *83*, 8462–8466. (c) Senear, D. F.; Brenowitz, M.; Shea, M. A.; Ackers, G. K. *Biochemistry* **1986**, *25*, 7344–7354.

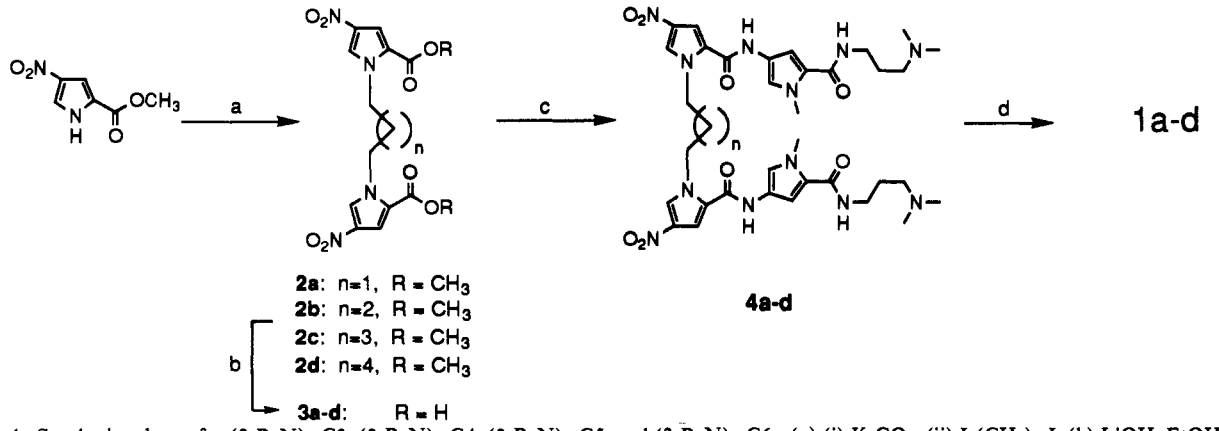

Figure 4. Synthetic scheme for (2-PyN)$_2$-C3, (2-PyN)$_2$-C4, (2-PyN)$_2$-C5, and (2-PyN)$_2$-C6. (a) (i) K_2CO_3; (ii) I-$(CH_2)_n$-I; (b) LiOH, EtOH, H_2O; (c) (i) $SOCl_2$; (ii) 1-methyl-4-amino-2-(carboxamidopropyl)-3-(dimethylamino)pyrrole; (d) (i) 300 psi H_2, 10% Pd/C; (ii) picolinic acid, DCC, HOBt.

amounts of peptide show a single complex forming, which is nearly identical for all five peptides. Two-dimensional NOESY experiments of the oligonucleotide complexed with 2 equiv of 2-PyN reveal that the monomer binds as a side-by-side dimer, similar to the characterized (2-ImN)$_2$·5′-TGACT-3′ complex.[12] Two-dimensional NOESY experiments of the oligonucleotide complexed with 1 equiv of either (2-PyN)$_2$-C3 or (2-PyN)$_2$-C6 reveal that the covalent peptide dimers do indeed bind as intramolecular dimers. Since the one-dimensional spectra are nearly identical for all the ligands, we infer that the butyl- and pentyl-linked peptides also bind as intramolecular dimers.[20] The NOESY crosspeaks are essentially identical in shift and intensity for all complexes, suggesting that the linked peptides bind with similar geometry and peptide–DNA contacts.[20]

Implications for the Design of Minor Groove-Binding Peptides. This first generation of covalently linked peptide dimers employing simple alkyl linkers binds to the minor groove of DNA at 5′-TGTCA-3′ sites with 10-fold higher binding affinities than does the parent peptide 2-PyN. In addition, the dimeric peptides bind double-helical DNA with improved sequence specificities. These results suggest that covalently linking peptides for side-by-side binding may be an important component in the rational design of peptides for sequence specific recognition of the minor groove of DNA. We would expect such an effect to be most evident with a heterodimeric system, wherein two different peptides can formally bind to three different binding sites: each of the parent sites and the heterodimer site.[14] A covalently linked heterodimer of two different peptides would be expected to display increased binding affinity for the heterodimer site and improved sequence specificity.

Experimental Section

^{1}H NMR and ^{13}C NMR spectra were recorded on a General Electric-QE 300 NMR spectrometer in $CDCl_3$ or DMSO-d_6, with chemical shifts reported in parts per million relative to tetramethylsilane or residual DMSO-d_5, respectively. IR spectra were recorded on a Perkin–Elmer FTIR spectrometer. High-resolution mass spectra (HRMS) were recorded using fast atom bombardment (FAB) techniques at the Mass Spectrometry Laboratory at the University of California, Riverside. Reactions were executed under an inert argon atmosphere. Reagent grade chemicals were used as received unless otherwise noted. Tetrahydrofuran (THF) was distilled under nitrogen from sodium/benzophenone ketyl. Dichloromethane (CH_2Cl_2) and triethylamine were distilled under nitrogen from powdered calcium hydride. Dimethylformamide (DMF) was purchased as an anhydrous solvent from Aldrich. Flash chromatography was carried out using EM science Kieselgel 60 (230–400) mesh.[21] Thin-layer chromatography was performed on EM Reagents silica gel plates (0.5-mm thickness). All compounds were visualized with shortwave ultraviolet light.

***N,N′*-(1,*n*-Dialkyl)bis[2-(carboxymethyl)-4-nitropyrrole] 2a–d (Exemplified with 2a).** To a solution of 2-carboxy-4-nitropyrrole methyl ester (90 mg, 0.529 mmol) in acetone (4.0 mL) was added potassium carbonate (175 mg, 1.27 mmol), and the resulting solution was allowed to stir at room temperature for 1 h. 1,3-Diiodopropane (36 μL, 0.313 mmol) was added, and the reaction mixture was heated to 65 °C for 6 h. The solution was cooled, and solvent was removed under reduced pressure. The residue was purified by flash column chromatography (2% MeOH in CH_2Cl_2) to afford **2a**.

2a: yield 73% (85 mg); ^{1}H NMR ($CDCl_3$) δ 7.68 (d, 1 H, J = 2.0 Hz), 7.41 (d, 2 H, J = 2.0 Hz), 4.46 (t, 4 H, J = 7.3 Hz), 3.86 (s, 6 H), 2.17 (m, 2 H); ^{13}C NMR ($CDCl_3$) δ 160.3, 135.6, 126.9, 122.1, 113.2, 51.9, 47.4, 32.3; IR (thin film) 3132 (w), 2952 (m), 1715 (s), 1538 (m), 1515 (s), 1463 (m), 1417 (m), 1317 (s), 1257 (m), 1204 (m), 1103 (m), 860 (s); FABMS m/e 380.0974 (M + H, 380.0968 calcd for $C_{15}H_{16}N_4O_8$).

2b: yield 80% (140 mg); ^{1}H NMR ($CDCl_3$) δ 7.69 (d, 2 H, J = 2.0 Hz), 7.43 (d, 2 H, J = 2.0 Hz), 4.42 (m, 4 H), 3.88 (s, 6 H), 1.86 (m, 4 H); ^{13}C NMR ($CDCl_3$) δ 160.4, 135.5, 126.9, 121.9, 113.3, 52.0, 49.4, 27.8; IR (thin film) 3123 (w), 2955 (m), 1698 (s), 1538 (m), 1505 (s), 1420 (m), 1387 (m), 1325 (s), 1304 (m), 1257 (m), 1193 (m), 1082 (m), 748 (m); FABMS m/e 394.1141 (M + H, 394.1125 calcd for $C_{16}H_{18}N_4O_8$).

2c: yield 83% (85 mg); ^{1}H NMR ($CDCl_3$) δ 7.65 (d, 2 H, J = 2.0 Hz), 7.42 (d, 2 H, J = 2.0 Hz), 4.36 (t, 4 H, J = 7.4 Hz), 3.87 (s, 6 H), 1.87 (m, 4 H), 1.39 (m, 2 H); ^{13}C NMR ($CDCl_3$) δ 160.4, 135.5, 126.7, 122.0, 113.2, 51.9, 49.9, 30.4, 23.2; IR (thin film) 3144 (w), 2955 (w), 1713 (s) , 1504 (s), 1421 (m), 1389 (m), 1319 (s), 1266 (m), 1221 (m), 1122 (w), 1082 (m); FABMS m/e 408.1300 (M + H, 408.1281 calcd for $C_{17}H_{20}N_4O_8$).

2d: yield 81% (92 mg); ^{1}H NMR ($CDCl_3$) δ 7.62 (d, 2 H, J = 2.0 Hz), 7.42 (d, 2 H, J = 2.0 Hz), 4.34 (t, 4 H, J = 7.3 Hz), 3.86 (s, 6 H), 1.81 (m, 4 H), 1.37 (m, 4 H); ^{13}C NMR ($CDCl_3$) δ 160.4, 135.5, 126.7, 122.0, 113.2, 51.9, 50.2, 30.8, 25.8; IR (thin film) 3142 (w), 3117 (w), 2924 (w), 1715 (s), 1504 (s), 1423 (m), 1388 (m), 1320 (s), 1279 (m), 1246 (m), 1196 (m), 1083 (m); FABMS m/e 422.1452 (M + H, 422.1438 calcd for $C_{18}H_{22}N_4O_8$).

***N,N′*-(1,*n*-Dialkyl)bis[4-nitropyrrole-2-carboxylic Acid] 3a–d (Exemplified with 3a).** To a flask charged with bispyrrole methyl ester **2a** (280 mg, 0.737 mmol) was added ethanol (4.0 mL) and

(20) Dwyer, T. J.; Geierstanger, B. H.; Mrksich, M.; Dervan, P. B.; Wemmer, D. E. *J. Am. Chem. Soc.*, following paper in this issue.

(21) Still, W. C.; Kahn, M.; Mitra, A. *J. Org. Chem.* **1978**, *40*, 2923–2925.

(22) Iverson, B. L.; Dervan, P. B. *Nucl. Acids Res.* **1987**, *15*, 7823–7830.

(23) Maxam, A. M.; Gilbert, W. S. *Methods in Enzymol.* **1980**, *65*, 499–560.

(24) Sambrook, J.; Fritsch, E. F.; Maniatis, T. *Molecular Cloning*; Cold Spring Harbor Laboratory: Cold Spring Harbor, NY, 1989.

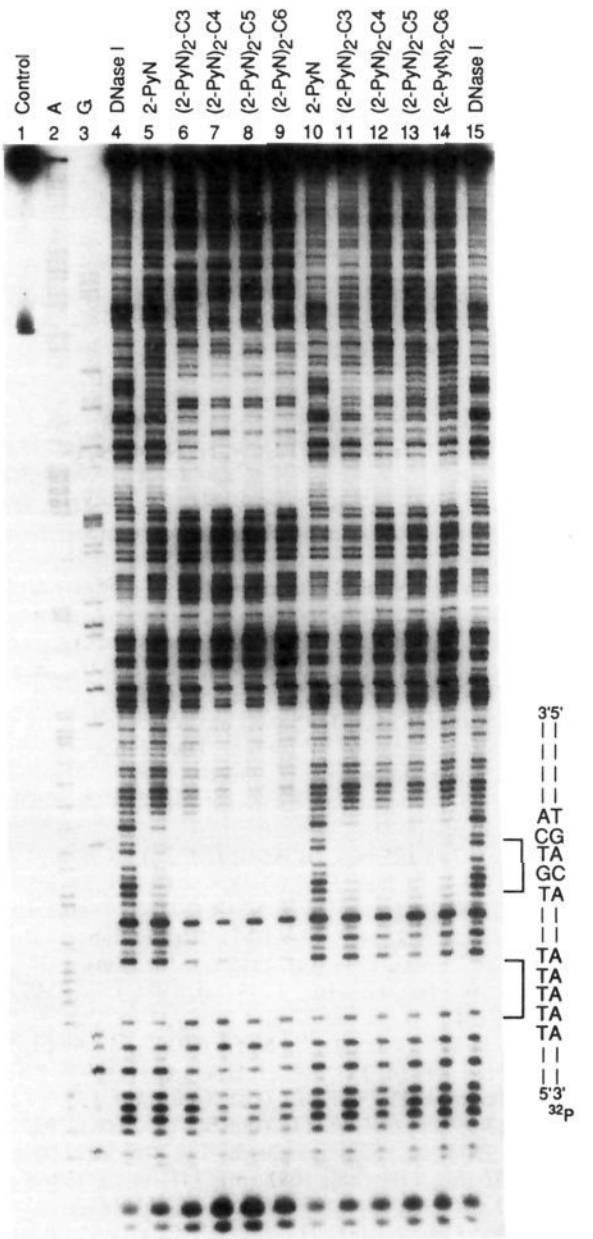

Figure 5. DNase I footprinting of 2-PyN, $(2\text{-PyN})_2$-C3, $(2\text{-PyN})_2$-C4, $(2\text{-PyN})_2$-C5, and $(2\text{-PyN})_2$-C6. The 5′-TGTCA-3′ and 5′-TTTTT-3′ binding sites are shown on the right side of the autoradiogram. All reactions contain 10 mM Tris·HCl, 10 mM KCl, 10 mM $MgCl_2$, 5 mM $CaCl_2$, and 100 μM-bp calf thymus DNA and 20 kcpm 3′-labeled 517-bp *Eco*R I/*Rsa* I restriction fragment from plasmid pBR322. Lane 1, intact DNA; lane 2, A reaction; lane 3, G reaction; lane 4, DNase I standard; lane 5, 40 μM 2-PyN; lane 6, 40 μM $(2\text{-PyN})_2$-C3; lane 7, 40 μM $(2\text{-PyN})_2$-C4; lane 8, 40 μM $(2\text{-PyN})_2$-C5; lane 9, 40 μM $(2\text{-PyN})_2$-C6; lane 10, 10 μM 2-PyN; lane 11, 10 μM $(2\text{-PyN})_2$-C3; lane 12, 10 μM $(2\text{-PyN})_2$-C4; lane 13, 10 μM $(2\text{-PyN})_2$-C5; lane 14, 10 μM $(2\text{-PyN})_2$-C6; lane 15, DNase I standard.

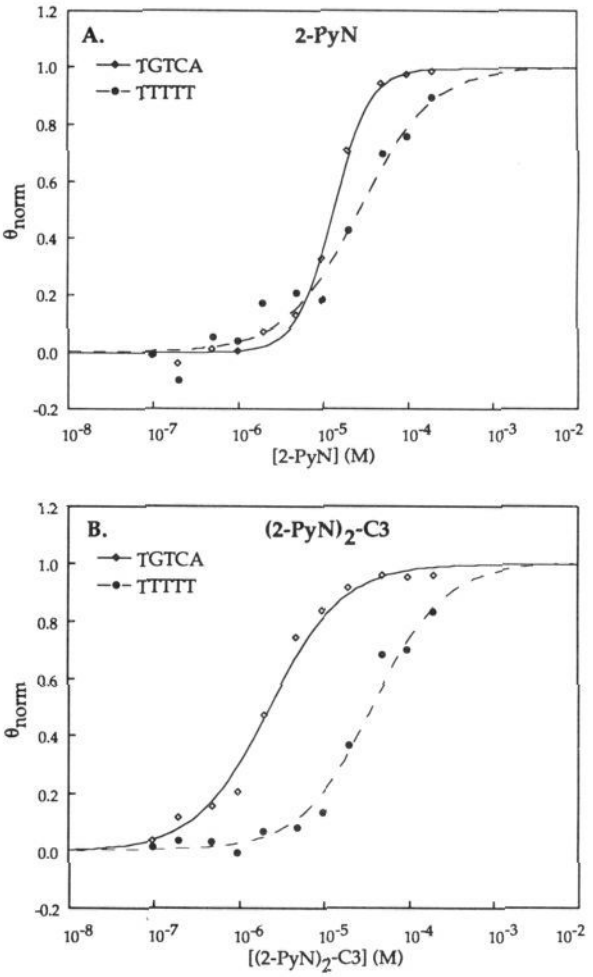

Figure 6. Data for the DNase I footprint titration experiments for (a) 2-PyN and (b) $(2\text{-PyN})_2$-C3 in complex with the 5′-TGTCA-3′ and 5′-TTTTT-3′ sites. The θ_{norm} points were obtained using photostimulable storage phosphor autoradiography and processed as described in the Experimental Section. The data points for the 5′-TGTCA-3′ site are indicated by open diamonds (◇) and for the 5′-TTTTT-3′ site by filled circles (●). The solid and dashed curves are the best-fit Langmuir binding titration isotherms obtained from nonlinear least squares algorithm using eq 2 ($n = 1$). The data points for 2-PyN binding the 5′-TGTCA-3′ site were fit with a modified Hill equation (eq 2).

0.5 N lithium hydroxide (8.0 mL). The mixture was heated to 80 °C and allowed to stir for 4 h. The solution was filtered, the pH of the filtrate was adjusted to pH = 2–3 with 1 N HCl, and the white precipitate was collected by filtration and dried to afford diacid **3a**.

3a: yield 93% (220 mg); ^{1}H NMR (DMSO-d_6) δ 8.28 (d, 2 H, J = 2.0 Hz), 7.25 (d, 2 H, J = 2.0 Hz), 4.39 (t, 4 H, J = 6.8 Hz), 2.22 (m, 2 H); ^{13}C NMR (DMSO-d_6) δ 160.9, 134.4, 128.8, 123.1, 112.0, 46.8, 31.7; IR (thin film) 3448 (w), 3178 (m), 2956 (w), 1700 (s), 1542 (m), 1515 (s), 1492 (m), 1421 (m), 1375 (s), 1301 (s), 1253 (m), 1207 (m), 1109 (m), 1082 (w), 860 (w), 817 (m), 752 (m); FABMS m/e 352.0661 (M + H, 352.0655 calcd for $C_{13}H_{13}N_4O_8$).

3b: yield 97% (320 mg); ^{1}H NMR (DMSO-d_6) δ 8.25 (s, 2 H), 7.24 (s, 2 H), 4.34 (bs, 4 H), 1.66 (bs, 4 H); ^{13}C NMR (DMSO-d_6) δ 160.8, 134.3, 128.7, 123.1, 112.0, 48.9, 27.4; IR (thin film) 3448 (w), 3138 (m), 2961 (w), 1686 (s), 1543 (m), 1508 (s), 1422 (m), 1372 (s), 1321 (s), 1264 (m), 1194 (m), 1101 (m), 1083 (w), 866 (w), 822 (m), 751 (m); FABMS m/e 367.0898 (M + H, 367.0890 calcd for $C_{14}H_{15}N_4O_8$).

3c: yield 95% (180 mg); ^{1}H NMR (DMSO-d_6) δ 8.24 (d, 2 H, J = 2.0 Hz), 7.25 (d, 2 H, J = 2.0 Hz), 4.33 (t, 4 H, J = 7.0 Hz), 1.72 (m, 4 H), 1.17 (m, 2 H); ^{13}C NMR (DMSO-d_6) δ 160.8, 134.2, 128.8, 123.0, 112.0, 49.1, 30.0, 22.5; IR (thin film) 3448 (w), 3140 (m), 2949 (w), 1684 (s), 1504 (m), 1510 (s), 1420 (m), 1371 (m), 1318 (s), 1272 (m), 1189 (w), 1098 (w), 861 (w) 754 (w); FABMS m/e 381.1047 (M + H, 381.1046 calcd for $C_{15}H_{17}N_4O_8$).

3d: yield 95% (600 mg); ^{1}H NMR (DMSO-d_6) δ 8.23 (d, 2 H, J = 2.0 Hz), 7.24 (d, 2 H, J = 2.0 Hz), 4.31 (t, 4 H, J = 7.0 Hz), 1.68 (bs, 4 H), 1.21 (bs, 4 H); ^{13}C NMR (DMSO-d_6) δ 160.8, 134.2, 128.8, 123.0, 112.0, 49.3, 30.4, 25.3; IR (thin film) 3448 (m), 3144 (m), 2945 (m), 1691 (s), 1509 (s), 1413 (s), 1380

(s), 1319 (s), 1285 (s), 1255 (s), 1195 (m), 1104 (w), 916 (m); FABMS *m/e* 395.1190 (M + H, 395.1202 calcd for $C_{16}H_{19}N_4O_8$).

***N*-Methyl-4-nitro-2-(carboxamidopropyl)-3-(dimethylamino)-pyrrole.** A suspension of *N*-methyl-4-nitropyrrole-2-carboxylic acid (4.0 g, 23.5 mmol) in thionyl chloride (10 mL, 137 mmol) was heated under reflux for 8 h. Excess thionyl chloride was removed *in vacuo*, and the acid chloride was dissolved in DMF (10 mL) and cooled to 0 °C. 3-Dimethylpropylamine (6.0 mL, 46.7 mmol) was slowly added, and the solution was allowed to warm to room temperature and stirred for 10 h. After addition of water (30 mL), the reaction mixture was partitioned between ethyl acetate (150 mL) and 10% $NaHCO_3$ (150 mL). The layers were separated, and the aqueous layer was washed once more with ethyl acetate (100 mL). The combined organic fractions were dried ($MgSO_4$), and the solvent was removed under reduced pressure to afford the nitropyrrole (5.20 g, 88%) as a white solid: ^{1}H NMR ($CDCl_3$) δ 8.86 (b, 1 H), 7.54 (d, 1 H, J = 1.9 Hz), 6.92 (d, 1 H, J = 1.9 Hz), 4.02 (s, 3 H), 3.51 (q, 2 H, J = 6.7 Hz), 2.52 (t, 2 H, J = 7.1 Hz), 2.32 (s, 6 H), 1.74 (q, 2 H, J = 7.2 Hz); ^{13}C NMR ($CDCl_3$) δ 160.5, 135.3, 128.0, 126.3, 106.4, 59.3, 45.3, 40.2, 37.8, 24.7; IR (thin film) 3126 (m), 2955 (m), 2793 (m), 1651 (s), 1548 (s), 1504 (s), 1454 (m), 1306 (s), 1210 (m), 1175 (m), 1138 (m), 1106 (m), 1039 (m), 987 (w), 909 (m).

***N*-Methyl-4-amino-2-(carboxamidopropyl)-3-(dimethylamino)-pyrrole.** A solution of *N*-methyl-4-nitro-2-(carboxamidopropyl)-3-(dimethylamino)pyrrole (4.00 g, 15.7 mmol) and Pd/C catalyst (10%, 600 mg) in DMF (30 mL) was hydrogenated (50 psi) in a shaker apparatus for 8 h. The mixture was filtered through celite to remove catalyst, and the solvent was removed under reduced pressure. The dark oil was quickly purified by flash column chromatography (0 to 1% ammonium hydroxide in methanol, gradient) to afford the product as a yellow oil (2.20 g, 62%). 4-Aminopyrroles are not very stable and are used immediately after purification in subsequent reactions: ^{1}H NMR (DMSO-d_6) δ 8.00 (s, 1 H), 7.30 (b, 1 H), 6.30 (s, 1 H), 3.69 (s, 3 H), 3.18, (q, 2 H, J = 6.1 Hz), 2.95 (t, 2 H, J = 7.5 Hz), 2.67 (s, 6 H), 1.81 (b, 2 H).

***N,N'*-(1,*n*-Dialkyl)bis[2,4-carboxamide-2-(carboxamidopropyl)-3-(dimethylamino)pyrrolyl]-4-nitropyrrole 4a–d (Exemplified with 4d).** A solution of diacid **3d** (430 mg, 1.09 mmol) in thionyl chloride (10.0 mL, 137 mmol) was heated under reflux for 6 h. Excess thionyl chloride was removed by distillation, and the crude acid chloride was dissolved in DMF (8.0 mL). To this was added a solution of *N*-methyl-4-amino-2-(carboxamidopropyl)-3-(dimethylamino)pyrrole (880 mg, 3.46 mmol) in DMF (10.0 mL), and the resulting solution was allowed to stir at room temperature for 3 h. Methanol (2.0 mL) was added, and the solvents were removed under reduced pressure. The crude residue was partitioned between ethyl acetate (100 mL) and 10% sodium bicarbonate (100 mL), the layers were separated, and the aqueous fraction was further washed with ethyl acetate (2 × 50 mL). The combined organic fractions were filtered through Celite and dried (Na_2SO_4), and the solvent was removed under reduced pressure and dried to afford bis-dipyrrole **4d** as a yellow powder. If necessary, the product can be purified by flash column chromatography (1–2% ammonium hydroxide in methanol, gradient).

4a: yield 65% (330 mg); ^{1}H NMR (DMSO-d_6) δ 10.23 (s, 2 H) 8.25 (d, 2 H, J = 1.7 Hz), 8.10 (b, 2 H), 7.60 (d, 2 H, J = 1.4 Hz), 7.16 (d, 2 H, J = 1.6 Hz), 6.74 (d, 2 H, J = 1.6 Hz), 4.45 (t, 4 H, J = 6.1 Hz), 3.16 (b, 4 H), 3.77 (s, 6 H), 2.24–2.29 (b, 2 H), 2.21 (t, 4 H, J = 7.0 Hz), 2.10 (s, 12 H), 1.58 (m, 4 H); ^{13}C NMR (DMSO-d_6) δ 161.4, 157.1, 134.7, 128.3, 126.2, 123.8, 121.8, 118.4, 108.5, 104.1, 57.5, 47.3, 45.7, 39.4, 37.5, 36.5, 27.7; FABMS *m/e* 765.3796 (M + H, 765.3796 calcd for $C_{35}H_{49}N_{12}O_8$).

4b: yield 86% (330 mg); ^{1}H NMR (DMSO-d_6) δ 10.24 (s, 2 H), 8.23 (d, 2 H, J = 1.8 Hz), 8.11 (t, 2 H, J = 5.5 Hz), 7.59 (d, 2 H, J = 1.5 Hz), 7.19 (d, 2 H, J = 1.7 Hz), 6.78 (d, 2 H, J = 1.7 Hz), 4.42 (b, 4 H), 3.79 (s, 6 H), 3.18 (m, 4 H), 2.21 (t, 4 H, J = 6.9 Hz), 2.10 (s, 12 H), 1.71 (b, 4 H), 1.58 (m, 4 H); ^{13}C NMR (DMSO-d_6) δ 161.4, 157.1, 134.5, 128.2, 126.3, 123.8, 121,8, 118.4, 108.5, 104.2, 57.6, 49.3, 45.7, 40.8, 36.5, 28.3, 27.7; FABMS *m/e* 779.3984 (M + H, 779.3953 calcd for $C_{36}H_{51}N_{12}O_8$).

4c: yield 70% (235 mg); ^{1}H NMR (DMSO-d_6) δ 10.24 (s, 2 H), 8.20 (d, 2 H, J = 1.9 Hz), 8.12 (t, 2 H, J = 5.8 Hz), 7.59 (d, 2 H, J= 1.9 Hz), 7.19 (d, 2 H, J = 1.8 Hz), 6.79 (d, 2 H, J = 1.8 Hz), 4.37 (t, 4 H, J = 6.9 Hz), 3.78 (s, 6 H), 3.16 (m, 4 H), 2.20 (m, 4 H), 2.10 (s, 12 H), 1.70 (b, 4 H), 1.58 (m, 4 H), 1.20 (b, 2 H); ^{13}C NMR (DMSO-d_6) δ 161.4, 157.1, 134.5, 128.0, 126.1, 123.8, 121.7, 118.4, 108.5, 104.2, 57.6, 49.6, 45.7, 37.4, 36.5, 30.9, 27.7, 23.2; FABMS *m/e* 793.4147 (M + H, 793.4109 calcd for $C_{37}H_{53}N_{12}O_8$).

4d: yield 56% (490 mg); ^{1}H NMR (DMSO-d_6) δ 10.24 (s, 2 H), 8.18 (d, 2 H, J = 1.8 Hz), 8.12 (t, 2 H, J = 5.4 Hz), 7.55 (d, 2 H, J = 1.6 Hz), 7.18 (d, 2 H, J = 1.6 Hz), 6.79 (d, 2 H, J = 1.7 Hz), 4.36 (t, 4 H, J = 6.7 Hz), 3.78 (s, 6 H), 3.16 (m, 4 H), 2.20 (t, 4 H, J = 7.0 Hz), 2.10 (s, 12 H), 1.70 (b, 4 H), 1.58 (m, 4 H), 1.22 (b, 4 H); ^{13}C NMR (DMSO-d_6) δ 161.5, 157.1, 134.4, 127.9, 126.2, 123.8, 121.8, 118.4, 108.4, 104.3, 57.6, 49.7, 45.7, 41.0, 36.5, 31.3, 27.7, 26.0; FABMS *m/e* 807.4224 (M + H, 807.4266 calcd for $C_{38}H_{55}N_{12}O_8$).

Bis(pyridine-2-carboxamidonetropsin)(CH$_2$)$_{3-6}$ 1a–d (Exemplified with 1d). To a solution of picolinic acid (58 mg, 0.47 mmol) and *N*-hydroxybenzotriazole hydrate (60 mg, 0.44 mmol) in DMF (1.0 mL) was added a solution of 1,3-dicyclohexylcarbodiimide (93 mg, 0.45 mmol) in CH_2Cl_2 (1.0 mL). The solution was allowed to stir for 30 min at room temperature. Separately, to a solution of bis-dipyrrole **4d** (62 mg, 0.077 mmol) in DMF (2.0 mL) was added palladium on activated carbon (10%, 37 mg), and this mixture was allowed to stir under a hydrogen atmosphere (300 psi) in a Parr bomb apparatus for 4 h. The reaction mixture was filtered through Celite and added to the activated acid. The resulting solution was allowed to stir for 2 h, and methanol (1.0 mL) was added. The solvents were removed under reduced pressure, the residue was partitioned between CH_2Cl_2 (50 mL) and 10% sodium bicarbonate (50 mL), the layers were separated, and the aqueous fraction was washed once more with CH_2Cl_2 (50 mL). The combined organic layers were dried (Na_2SO_4), and the solvent was removed under reduced pressure. This residue was further purified by flash column chromatography (2% ammonium hydroxide in methanol) to afford the covalent peptide dimer **1d** as a yellow powder.

1: yield 55% (38 mg); ^{1}H NMR ($CDCl_3$) δ 9.55 (s, 2 H), 8.42 (d, 2 H, J = 4.2 Hz), 8.23 (d, 2 H, J = 7.8 Hz), 8.08 (m, 4 H), 7.91 (dt, 2 H, J = 7.6 Hz, J = 1.7 Hz), 7.45 (dt, 2 H, J = 4.7 Hz, J = 1.1 Hz), 7.28 (d, 2 H, J = 1.6 Hz), 6.95 (d, 2 H, J = 1.6 Hz), 6.55 (d, 2 H, J = 1.7 Hz), 6.43 (d, 2 H, J = 1.7 Hz), 4.40 (b, 4 H), 3.87 (s, 6H), 3.48 (m, 2 H), 2.46 (t, 4 H, J = 6.4 Hz), 2.34 (bs, 2 H), 2.30 (s, 12 H), 1.79 (m, 4 H); ^{13}C NMR ($CDCl_3$) δ 162.1, 161.9, 158.7, 149.5, 148.0, 137.5, 126.2, 123.6, 123.5, 122.1, 121.7, 120.2, 118.5, 118.2, 105.8, 102.1, 58.7, 47.5, 45.3, 39.1, 36.6, 31.0, 26.1; IR (thin film) 3299 (m), 2940 (w), 1651 (s), 1584 (m), 1540 (s), 1464 (m), 1436 (m), 1403 (m), 1260 (m), 1118 (w), 1087 (w); UV (H_2O) λ_{max} (ϵ) 244 (33 300), 306 (40 000) nm, (CH_3CN) λ_{max} (ϵ) 242 (38 400), 302 (46 100) nm; FABMS *m/e* 915.4704 (M + H, 915.4704 calcd for $C_{47}H_{58}N_{14}O_6$).

1b: yield 54% (33 mg); ^{1}H NMR ($CDCl_3$) δ 9.56 (s, 2 H), 8.41 (d, 2 H, J = 4.7 Hz), 8.26 (d, 2 H, J = 2.2 Hz), 8.15 (t, 2 H, J = 4.8 Hz), 8.06 (s, 2 H), 7.93 (t, 2 H, J = 7.6 Hz), 7.47 (t, 2 H, J = 5.6 Hz), 7.31 (s, 2 H), 6.96 (s, 2 H), 6.59 (s, 2 H), 6.43 (s, 2H), 4.29 (bs, 4 H), 3.88 (s, 6 H), 3.48 (q, 4 H, J = 5.5 Hz), 2.44 (t, 4 H, J = 6.3 Hz), 2.33 (m, 2 H), 2.29 (s, 12 H), 1.77 (m, 4 H), 1.66 (bs, 4 H); ^{13}C NMR ($CDCl_3$) δ 162.0, 161.9,

158.6, 149.5, 148.0, 137.6, 126.2, 124.0, 123.6, 122.2, 121.6, 120.4, 118.6, 105.1, 101.9, 96.1, 58.8, 47.7, 45.4, 39.1, 36.7, 27.4, 26.2; IR (thin film) 3304 (m), 2942 (w), 1651 (s), 1588 (m), 1538 (s), 1463 (m), 1435 (m), 1403 (m), 1261 (m), 1120 (w), 1089 (w); UV (H_2O) λ_{max} (ϵ) 242 (30 200), 308 (34 300) nm, (CH_3CN) λ_{max} (ϵ) 242 (34 100), 302 (42 800) nm; FABMS *m/e* 929.4919 (M + H, 929.4899 calcd for $C_{48}H_{60}N_{14}O_6$).

1c: yield 43% (30 mg); ^{1}H NMR ($CDCl_3$) δ 9.59 (s, 2 H), 8.48 (d, 2 H, J = 4.8 Hz), 8.29 (d, 2 H, J = 7.9 Hz), 8.22 (s, 1 H), 8.14 (b, 1 H), 7.95 (td, 2 H, J = 7.7 Hz, J = 1.5 Hz), 7.49 (t, 2 H, J = 6.2 Hz), 7.35 (d, 2 H, J = 1.6 Hz), 7.03 (d, 2 H, J = 1.6 Hz), 6.57 (d, 2 H, J = 1.7 Hz), 6.53 (d, 2 H, J = 1.7 Hz), 4.29 (t, 4 H, J = 5.8 Hz), 3.91 (s, 3 H), 3.48 (q, 4 H, J = 5.0 Hz), 2.45 (t, 4 H, J = 6.4 Hz), 2.29 (s, 6 H), 1.77 (m, 2 H), 1.62 (m, 2 H), 0.83 (m, 2 H); ^{13}C NMR ($CDCl_3$) δ 161.9, 161.8, 158.8, 149.6, 148.1, 137.7, 126.3, 124.1, 123.6, 122.1, 121.8, 120.4, 118.5, 118.0, 104.5, 102.1, 58.9, 48.0, 45.4, 39.2, 36.7, 26.1, 21.5; IR (thin film) 3294 (m), 2943 (w), 1645 (s), 1578 (m), 1538 (s), 1464 (m), 1431 (m), 1404 (m), 1268 (m), 1120 (w), 1079 (w); UV (H_2O) λ_{max} (ϵ) 244 (30 700), 302 (33 500) nm, (CH_3CN) λ_{max} (ϵ) 242 (35 400), 302 (42 000) nm; FABMS *m/e* 943.5032 (M + H, 943.5055 calcd for $C_{49}H_{62}N_{14}O_6$).

1d: yield 61% (45 mg); ^{1}H NMR ($CDCl_3$) δ 9.70 (s, 2 H), 8.51 (d, 2 H, J = 4.0 Hz), 8.26 (d, 2 H, J = 7.8 Hz), 8.17 (s, 2 H), 7.97 (t, 2 H, J = 4.5 Hz), 7.89 (td, 2 H, J = 7.7 Hz, J = 1.3 Hz), 7.45 (t, 2 H, J = 6.0 Hz), 7.29 (d, 2 H, J = 1.6 Hz), 7.16 (d, 2 H, J = 1.6 Hz), 6.73 (d, 2 H, J = 1.6 Hz), 6.54 (d, 2 H, J = 1.6 Hz), 4.32 (t, 4 H, J = 6.0 Hz), 3.89 (s, 6 H), 3.45 (q, 2 H, J = 5.8 Hz), 2.44 (t, 4 H, J = 6.4 Hz), 2.33 (bs, 2 H), 2.29 (s, 12 H), 1.75 (m, 4 H), 1.68 (b, 4 H), 1.10 (b, 4 H); ^{13}C NMR ($CDCl_3$) δ 161.8, 161.5, 158.8, 149.5, 148.0, 137.7, 126.2, 123.5, 123.1, 122.1, 121.6, 120.7, 118.6, 117.9, 104.1, 102.5, 58.7, 48.9, 45.3, 39.1, 36.6, 30.9, 26.4, 26.0; IR (thin film) 3313 (m), 2940 (w), 1652 (s), 1584 (m), 1538 (s), 1464 (m), 1435 (m), 1404 (m), 1262 (m), 1121 (w), 1088 (w); UV (H_2O) λ_{max} (ϵ) 244 (30 100), 304 (34 200) nm, (CH_3CN) λ_{max} (ϵ) 242 (35 400), 302 (40 000) nm; FABMS *m/e* 957.5181 (M + H, 957.5212 calcd for $C_{50}H_{64}N_{14}O_6$).

DNA Reagents and Materials. Doubly distilled water was further purified through the Milli Q filtration system from Millipore. Sonicated, deproteinized calf thymus DNA was purchased from Pharmacia. Plasmid pBR322 was obtained from Boehringer-Mannheim. Enzymes were obtained from Boehringer-Mannheim or New England Biolabs and used with the buffers supplied. Deoxyadenosine 5′-[α-^{32}P]triphosphate was obtained from Amersham. Storage phosphor technology autoradiography was performed using a Molecular Dynamics 400S Phosphorimager and ImageQuant software. The 517 base pair 3′-end labeled *Eco*R I/*Rsa* I restriction fragment from plasmid pBR322 was prepared and purified as previously described.[11] Chemical sequencing reactions were performed according to published methods.[22,23] Standard techniques were employed for DNA manipulations.[24] All other reagents and materials were used as received.

Sample Preparation. Milligram quantities of peptide were placed in tared eppendorf tubes, dried at 1 Torr for 2 days, and immediately weighed. The peptides were dissolved in water, and the extinction coefficients were determined from the absorbances as measured on a Hewlett Packard 8452A diode array spectrophotometer. Reported extinction coefficients represent the average of two determinations. Aqueous solutions of peptides were aliquoted into eppendorf tubes, lyophilized, and stored at −20 °C. The peptides were dissolved in water and serially diluted before each set of experiments.

DNase I Footprinting. All reactions were executed in a total volume of 10 μL with final concentrations of each species as indicated. The ligands were added to solutions of radiolabeled restriction fragment (20 000 cpm), calf thymus DNA (100 μM bp), Tris·HCl (10 mM, pH 7.0), KCl (10 mM), $MgCl_2$ (10 mM), and $CaCl_2$ (5 mM) and incubated for 15 min at 22 °C. Footprinting reactions were initiated by the addition of 1-μL stock solution of DNase I (10 units/mL) containing 1 mM dithiothreitol and allowed to proceed for 3 min at 22 °C. The reactions were stopped by addition of a 3 M ammonium acetate solution containing 250 mM EDTA and ethanol precipitated. The reactions were resuspended in 100 mM tris-borate-EDTA/80% formamide loading buffer and electrophoresed on 8% polyacrylamide denaturing gels (5% cross-link, 7 M urea) at 1000 V for 3–4 h.

DNase I Footprint Titration. Apparent first-order binding constants were determined by DNase I footprint titration as previously described.[16,19] The above reaction conditions were employed with ligand concentrations ranging from 200 μM to 100 nM. The footprint titration gels were dried and quantitated using storage phosphor technology. The data were analyzed by performing volume integrations of the 5′-TGTCA-3′ and 5′-TTTTT-3′ target sites and a 5′-GCGG-3′ reference site. The apparent DNA target site saturation, θ_{app}, was calculated for each concentration of peptide using the following equation:

$$\theta_{app} = 1 - \frac{I_{tot}/I_{ref}}{I_{tot^\circ}/I_{ref^\circ}} \quad (1)$$

where I_{tot} and I_{ref} are the integrated volumes of the target and reference sites, respectively, and I_{tot° and I_{ref° correspond to those values for a DNase I control lane to which no peptide has been added. At higher concentrations of peptide (>50 μM), the reference sites become partially protected, resulting in low θ_{app} values. For these data points, the reference values (I_{ref}) were corrected by multiplying the amount of radioactivity loaded per lane (CPM_{tot}) by the mean ratio of I_{ref}/CPM_{tot} for all data points from lanes with <50 μM peptide. The ([L], θ_{app}) data points were fit to a Langmuir binding isotherm (eq 2 n = 1) by minimizing the difference between θ_{app} and θ_{fit}:

$$\theta_{fit} = \theta_{min} + (\theta_{max} - \theta_{min})\frac{K_a^n[L]^n}{1 + K_a^n[L]^n} \quad (2)$$

where [L] corresponds to the total peptide concentration, K_a corresponds to the apparent monomeric association constant, and θ_{min} and θ_{max} represent the experimentally determined site saturation values when the site is unoccupied or saturated, respectively. Data were fit using a nonlinear least-squares fitting procedure of KaleidaGraph software (version 2.1, Abelbeck software) running on a Macintosh IIfx computer with K_a, θ_{max}, and θ_{min} as the adjustable parameters. The goodness-of-fit of the binding curve to the data points is evaluated by the correlation coefficient, with $R > 0.97$ as the criterion for an acceptable fit. Three sets of acceptable data were used in determining each association constant. The data were normalized using the following equation:

$$\theta_{norm} = \frac{\theta_{app} - \theta_{min}}{\theta_{max} - \theta_{min}} \quad (3)$$

The best fit binding isotherms for 2-PyN binding to the 5′-TGTCA-3′ site consistently give much worse fits than the other complexes. Visual inspection of the binding curves reveals that the increase in θ_{app} near half-saturation of the site is steeper than expected from the fitted curve, consistent with cooperative dimeric binding to this sequence by the peptides.[11,12] The footprint titration data cannot distinguish between binding by preassociated dimers and stepwise binding by two free peptides.[16] Therefore, these data were fit to a modified Hill equation (eq 2) with θ_{min}, θ_{max}, K_a, and n as adjustable parameters. For all data sets, the best fit value of n was in the range of 1.9–2.0, consistent with cooperative dimeric binding by the peptides.[16] We note explicitly that treatment of the data in this manner does not represent an

attempt to model a binding mechanism. Rather, we have chosen to compare relative values of K_a, the apparent first-order binding affinity, because this parameter represents the concentration of peptide at which the binding site is half-saturated.

Quantitation by Storage Phosphor Technology Autoradiography. Photostimulable storage phosphor imaging plates (Kodak Storage Phosphor Screen S0230 obtained from Molecular Dynamics) were pressed flat against gel samples and exposed in the dark at 22 °C for 15–20 h. A Molecular Dynamics 400S PhosphorImager was used to obtain all data from the storage screens. The data were analyzed by performing volume integrations of all bands using the ImageQuant version 3.0 software running on an AST Premium 386/33 computer.

Acknowledgment. We are grateful to the National Institutes of Health (GM-27681) and National Foundation for Cancer Research for research support and a National Institutes of Health Research Service Award to M.M.